Effect of Bin Time on the Photon Counting Histogram for One-Photon Excitation

Thomas D. Perroud, Bo Huang, and Richard N. Zare*[a]

We have demonstrated that our photon counting histogram (PCH) model with the correction for one-photon excitation is valid at multiple bin times. The fitted apparent brightness and concentration follow the three-dimensional diffusion model. More importantly, the semi-empirical parameter, F, introduced in the PCH model for one-photon excitation to correct for the non-Gaussian shape of the observation volume, shows small variations with different bin times. These variations are consistent with the physical interpretation of F, and they do not affect the resolving power of the PCH model for one-photon excitation. Based on these findings, we extend the time-independent PCH analysis to time-dependent photon counting multiple histograms (PCMH). This model considers the effect of bin time on the PCH parameters in a way that is similar to fluorescence intensity multiple distribution analysis (FIMDA). From the same set of data, PCMH extracts time-dependent parameters (diffusion time and triplet-state relaxation time) as well as time-independent parameters (true specific brightness and true average number of molecules). Given a three- to fourfold experimental difference in molecular brightness, we find that PCMH can resolve each species in a two-species sample and extract their respective diffusion times even when fluorescence correlation spectroscopy cannot.

Introduction

For optimum signal-to-noise and data collection efficiency, it is often advantageous to record the fluctuations in count rate from several molecules rather than one. This approach is called few-molecule spectroscopy[1] (also aptly called fluorescence fluctuation spectroscopy). Biological problems addressed by fluorescence fluctuation spectroscopy include the memory effect observed in horseradish peroxidase,[2] conformational changes of DNA,[3] the photophysics of green fluorescent proteins,[4] diffusion within a membrane,[5] and receptor–ligand binding.[6]

The fluctuations in a fluorescence signal can be divided into two components: the fluctuations with time and the fluctuations in signal amplitude. The well-established technique of fluorescence correlation spectroscopy (FCS) makes use of fluctuations with time.[7–9] Fluctuations in amplitude have only recently been the subject of attention. Techniques to analyze them include analysis of fluctuation moments,[10,11] the photon counting histogram (PCH) model,[12] fluorescence intensity distribution analysis (FIDA),[13] and fluorescence cumulant analysis.[14] These techniques characterize each fluorescent species by two parameters: the molecular brightness, which we denote by ε and the average number of particles in the observation volume, which we denote by $\bar{N}$. Recently the PCH analysis has been extended to one-photon excitation for confocal spectroscopy.[1,15]

PCH and FIDA focus on the fluctuations of the fluorescence signal amplitude while discarding all time-correlated information. In 2000, Palo et al.[16] pointed out that processes occurring on the time scale of the bin time affect the values of the parameters determined by FIDA. Such processes include molecular diffusion out of or into the observation volume, photophysical processes (triplet-state formation), and isomerization. Thus FIDA can only determine an apparent molecular brightness and apparent concentration for a fluorescent species. To correct for this and to obtain the true parameters, Palo et al. extended FIDA to fluorescence intensity multiple distribution analysis (FIMDA). By analyzing distributions with multiple bin times, they were able to obtain simultaneously the true molecular brightness and the diffusion time of a fluorescent species from a single data set. Although FIDA and PCH are mathematically equivalent in describing the photon statistics, they differ in the treatment of the observation volume, which deviates from a three-dimensional (3D) Gaussian function when using one-photon excitation.[13,15] FIDA uses a purely empirical approach through a polynomial function with two or three parameters. PCH for one-photon excitation uses a correction based on an understanding of the deviation from a 3D Gaussian approximation. By introducing a semi-empirical parameter *F*, the PCH model takes into account the out-of-focus emission responsible for the non-Gaussian nature of the observation volume profile. The robustness of this correction method has been tested with different dyes and instrumental configurations.[1,15] In this article, we test the robustness and validity of PCH for one-photon excitation at variable bin times by studying the effect of bin time on $\bar{N}$, ε, and especially the *F* factor. Herein we determine the optimum bin time for PCH analysis, and also introduce a variant of the PCH model called photon counting multiple histograms (PCMH) similar to FIMDA.

Theory

In this section we first review the theory of one-photon PCH of freely diffusing molecules for bin times shorter than the time

[a] *T. D. Perroud, B. Huang, Prof. Dr. R. N. Zare*
Department of Chemistry, Stanford University, Stanford
California 94305-5080 (USA)
Fax: (+1) 650-723-9262
E-mail: zare@stanford.edu

 DOI: 10.1002/cphc.200400547

scale of the process of interest. We then develop an expression relating the time-independent PCH model to the time-dependent FCS theory. This expression allows us to relate PCH to parameters characterizing time-dependent processes.

The PCH Model

The PCH technique accounts for the fluctuations in fluorescence amplitude caused by molecules diffusing through an observation volume. For an integration time T shorter than the time scale of a particular process, PCH characterizes each fluorescent species by two parameters: the average number of particles in the observation volume V, denoted by $\bar{N}$, and the molecular brightness, denoted by ε (counts per bin time per molecule). According to the PCH model, the probability p of detecting k photon counts ($k>0$) from a single fluorescent particle in a fixed bin time and in a sufficiently large reference volume QV is given by Equation (1):

$$p^{(1)}(k;Q,\varepsilon) = \frac{1}{QV}\int \text{Poisson}[k,\varepsilon \cdot W(\vec{r})]\mathrm{d}\vec{r} \quad (1)$$

where $W(\vec{r})$ is the actual observation volume profile, Q (arbitrarily set to 6 in our calculations) is the ratio between the reference volume QV and the volume of observation V, and Poisson(k,x) is the Poisson distribution for k objects having a mean of x.

As previously shown,[15] the observation volume profile cannot be approximated by a three-dimensional Gaussian function, $W_{3DG}(\vec{r})$, for the PCH model in the case of one-photon excitation. To correct for this failure, we introduced a semi-empirical parameter[1] F_j, defined as the relative difference between the integral of the jth power of the actual observation volume profile, $W(\vec{r})$, and that of its 3D Gaussian approximation, $W_{3DG}(\vec{r})$. Equation (1) becomes Equation (2):

$$p^{(1)}(k;Q,\varepsilon) = \frac{1+F_2}{(1+F_1)^2}\left[p_G^{(1)}(k;Q,\varepsilon) + \frac{1}{Qk!}\sum_{j=k}^{\infty}\frac{(-1)^{j-k}}{(j-k)!(2j)^{\frac{3}{2}}}\varepsilon^j F_j\right] \quad (2)$$

Depending on experimental conditions, a second-order correction may be needed, $j\leq 2$. For all the results presented herein, a second-order correction did not improve the goodness of the fit, and thus we only used a first-order correction, $F_1=F$, to fit all histograms. The parameter F characterizes the shape of the observation volume for a confocal microscope by being the ratio of the out-of-focus background to the in-focus signal. It gives the extent of the deviation from a 3D Gaussian observation volume, so that, when F approaches zero, the actual volume of observation is a 3D Gaussian volume.

Assuming noninteracting particles, the probability of detecting k photon counts from N fluorescent particles, $p^{(N)}(k;Q,\varepsilon)$, is given by convoluting N times the probability of a single fluorescent particle, $p^{(1)}(k;Q,\varepsilon)$. If we account for the fluctuations in the number of particles within the reference volume QV, which is governed by Poisson statistics, the probability is expressed by Equation (3):

$$P(k;\bar{N},\varepsilon) = \sum_{N=0}^{\infty} p^{(N)}(k;Q,\varepsilon)\cdot \text{Poisson}(N,Q\bar{N}) \quad (3)$$

where $P(k;\bar{N},\varepsilon)$ is the PCH for a fluorescent species characterized by a molecular brightness ε. The PCH for multiple species, each characterized by a different molecular brightness, is the convolution of the PCH functions for the individual species.

A brief note on the convention chosen for the average number of particles in the observation volume, $\bar{N}$, will be helpful at the outset. For both FCS and PCH, we choose to define $\bar{N}$ as the reciprocal of the correlation amplitude in the case of three-dimensional diffusion. The size of the observation volume, V, that corresponds to this definition of $\bar{N}$ is given by Equation (4):

$$V = \frac{\omega_1^2}{\omega_2} \quad (4)$$

where [Eq. (5)]:

$$\omega_j = \int [W(\vec{r})]^j \mathrm{d}\vec{r} \quad (5)$$

Under the experimental conditions of high fluorescence intensity and/or small integration time, the nonideal behavior of the detector must be considered. Hillesheim and Müller[17] have shown that the nonideal behavior of the photodetector arises largely from its dead time, τ_{Dead}, defined as the minimum time interval between two consecutive photons needed to detect them as individual events. To correct for this nonideal behavior, they expressed the dead-time-modified PCH, $P'(k;\bar{N},\varepsilon,\delta)$, as a function of ideal PCHs, $P(k;\bar{N},\varepsilon)$, and $\delta=\tau_{Dead}/T$; see Equation (6):

$$P'(k;\bar{N},\varepsilon,\delta) = \sum_{j=0}^{k} P(j;\varepsilon(1-k\delta),\bar{N}) - \sum_{j=0}^{k-1} P(j;\varepsilon(1-(k-1)\delta),\bar{N}) \quad (6)$$

Hillesheim and Müller have also shown that the effect of afterpulses becomes significant when both ε and $\bar{N}$ are low (below 20000 counts per molecule per second, and below one molecule, respectively). We do not operate under these experimental conditions because of poor signal statistics, and thus the effect of afterpulses is considered as negligible.

Relating PCH to FCS

In the PCH model, Chen et al.[12] introduced a specific brightness, $\varepsilon_{sec}=\varepsilon/T$ (counts per second per molecule), that is independent of the arbitrary bin time T and allows for more convenient comparison between experiments. If PCH analysis were truly independent of the bin time, then $\bar{N}$ and ε_{sec} would remain constant regardless of the bin time used. In reality, these parameters are time-independent only if the integration time T is shorter than the time scale of the process of interest. Indeed as T approaches zero, PCH always obtains the true con-

centration, $\bar{N}_0=\bar{N}(0)$, and the true specific brightness, $\varepsilon_{sec}(0)$. Because we are considering the variation of $\bar{N}$ and ε_{sec} over a wide range of time scales, we define an apparent specific brightness, $\varepsilon_{sec}(T)$, and an apparent average number of molecules, $\bar{N}(T)$, that depend on the integration time T. In this section, we will show how $\bar{N}(T)$ and $\varepsilon_{sec}(T)$ can be related to $\bar{N}(0)$ and $\varepsilon_{sec}(0)$ in a fashion similar to the derivation of FIMDA.[16]

In a photon counting experiment with a fluctuating light source, Equation (7) gives the probability of observing k photon counts during an integration time T:

$$p(k,t,T) = \text{Poisson}(k, \int_t^{t+T} I(t)\mathrm{d}t) \tag{7}$$

When the light intensity $I(t)$ is constant, the distribution of photon counts is Poissonian. This fundamental form of noise is known as the shot noise. In reality, the light reaching the photodetector behaves in a stochastic way and the distribution of photon counts is a conditional probability distribution. The condition is based on the knowledge of the exact value of the integrated intensity $I(t)$. Thus, the statistical properties of this doubly stochastic Poisson process are completely specified when the statistical properties of $I(t)$ are given. Saleh[18] related the factorial moment of the photon count distribution, $p(k,t,T)$, to the moment of the intensity distribution. Similarly, we relate the first two factorial cumulants, $K_1(T)$ and $K_2(T)$, of $p(k,t,T)$ to the first two cumulants of $I(t)$ in Equations (8) and (9):

$$K_1(T) = \langle I\rangle T \tag{8}$$

$$K_2(T) = \int_{t_1}^{t_1+T}\int_{t_2}^{t_2+T}\left(\langle I(t_1)I(t_2)\rangle - \langle I\rangle^2\right)\mathrm{d}t_2\mathrm{d}t_1 \tag{9}$$

When the fluctuations of $I(t)$ are caused by stationary processes, the fluorescence autocorrelation function, $G(\tau)$, used in FCS[9] is given by Equation (10):

$$G(\tau) = \frac{1}{\bar{N}_0}g_x(\tau) = \frac{\langle \delta I(t)\delta I(t+\tau)\rangle}{\langle I\rangle^2} = \frac{\langle I(t)I(t+\tau)\rangle}{\langle I\rangle^2} - 1 \tag{10}$$

Here $g_x(\tau)$ is the solution of the autocorrelation function for a process x that gives rise to the fluctuations. We can then relate the second factorial cumulant to $g_x(\tau)$ [Eq. (11)]:

$$K_2(T) = \frac{\langle I\rangle^2 T^2}{\bar{N}_0}\Gamma(T) \tag{11}$$

where [Eq. (12)]

$$\Gamma(T) = \frac{1}{T^2}\int_{t_1}^{t_1+T}\int_{t_2}^{t_2+T} g_x(t_2-t_1)\mathrm{d}t_2\mathrm{d}t_1 \tag{12}$$

is defined for convenience.

Based on the analysis of fluctuation moments by Qian and Elson,[11] we relate the first and second factorial cumulants of the photon count distribution to $\varepsilon_{sec}(T)$ and $\bar{N}(T)$ [Eqs. (13) and (14)]:

$$K_1(T) = \gamma_2\bar{N}(T)\varepsilon_{sec}(T)T \tag{13}$$

$$K_2(T) = \gamma_2^2\bar{N}(T)[\varepsilon_{sec}(T)]^2T^2 \tag{14}$$

where $\gamma_2=\omega_2/\omega_1$. An additional γ_2 factor appears in Equations (13) and (14) because $\bar{N}$ refers to a volume that equals ω_1^2/ω_2 (instead of ω_1 as used by Qian and Elson).

Combining Equations (8), (11), (13), and (14), we obtain the time dependence of $\varepsilon_{sec}(T)$ and $\bar{N}(T)$ [Eqs. (15) and (16)]:

$$\varepsilon_{sec}(T) = \varepsilon_{sec}(0)\cdot\Gamma(T) \tag{15}$$

$$\bar{N}(T) = \frac{\bar{N}(0)}{\Gamma(T)} \tag{16}$$

where $\Gamma(T)$ can be calculated for any specific autocorrelation function $g_x(T)$. These equations, which we call PCMH curves, relate the variation in the apparent specific brightness $\varepsilon_{sec}(T)$ to its true value $\varepsilon_{sec}(0)$ [and similarly for relating $\bar{N}(T)$ to $\bar{N}(0)$].

Three-Dimensional Diffusion

The solution of the autocorrelation function $g_{Diff}(\tau)$ for the three-dimensional diffusion model in FCS[9] is expressed by Equation (17):

$$g_{Diff}(\tau) = \left(1+\frac{|\tau|}{\tau_{Diff}}\right)^{-1}\left(1+\frac{|\tau|}{\kappa^2\tau_{Diff}}\right)^{-1/2} \tag{17}$$

where τ_{Diff} is the diffusion time and κ is the geometry factor that describes the shape of the observation volume. We evaluate the corresponding $\Gamma_{Diff}(\tau)$ by substituting $g_{Diff}(\tau)$ into Equation (12); see Equation (18):

$$\Gamma_{Diff}(\tau) = \frac{4\kappa\tau_{Diff}}{\tau^2\sqrt{\kappa^2-1}}\left[(\tau_{Diff}+\tau)\tanh^{-1}\left(\frac{\sqrt{\kappa^2-1}\left(\sqrt{\kappa^2+\tau/\tau_{Diff}}-\kappa\right)}{1+\kappa\sqrt{\kappa^2+\tau/\tau_{Diff}}-\kappa^2}\right)\right. \tag{18}$$
$$\left.+\tau_{Diff}\sqrt{\kappa^2-1}\left(\kappa-\sqrt{\kappa^2+\tau/\tau_{Diff}}\right)\right]$$

Additional Fluctuation Processes

In addition to the diffusion of molecules through the observation volume, processes such as triplet-state formation or isomerization can contribute to fluctuations in fluorescence intensity. These processes usually occur on a time scale faster than diffusion, and therefore they are significant only at short bin times ($<10\,\mu s$). If a triplet is present, Widengren, Mets, and Rigler[19] suggested the following modification to the autocorrelation function in FCS [Eq. (19)]:

$$G(\tau) = \frac{1}{\bar{N}_0}g_{Diff}(\tau)\cdot g_{Trip}(\tau) \tag{19}$$

where the triplet blinking, $g_{Trip}(\tau)$, is described by a simple exponential decay given by Equation (20):

$$g_{Trip}(\tau) = 1 + \frac{F_{Trip} e^{-|\tau|/\tau_{Trip}}}{1-F_{Trip}} \quad (20)$$

Here τ_{Trip} is defined as the relaxation time between the dark state and the bright state, and F_{Trip} is defined as the average fraction of molecules in the dark state. Note that we choose Equation (20) to describe the triplet blinking so that $\bar{N}(0)$ in Equation (16) represents the average number of molecules in both the singlet and triplet states, and $\varepsilon_{sec}(0)$ in Equation (15) represents the averaged brightness for a molecule switching between the triplet and singlet states.

For immobilized molecules undergoing singlet–triplet blinking, we can evaluate the corresponding $\Gamma_{Trip}(\tau)$ from Equations (12) and (20); see Equation (21):

$$\Gamma_{Trip}(\tau) = 1 + \frac{2F_{Trip}\tau_{Trip}}{\tau(1-F_{Trip})}\left(1-\frac{\tau_{Trip}}{\tau}\left(1-e^{-\tau/\tau_{Trip}}\right)\right) \quad (21)$$

In FCS the overall solution of the autocorrelation function, including both triplet-state formation and 3D diffusion, is given by the product of the solution of each individual process [see Eq. (19)]. For PCMH, we need to integrate this product, which leads to a complicated solution. In most experimental cases, however, each process generates fluctuations in the fluorescence intensity on very different time scales ($\tau_{Trip} \ll \tau_{Diff}$). In other words, at short bin times, $\Gamma_{Trip}(\tau)$ dominates while $\Gamma_{Diff}(\tau)$ is unity (and vice versa for long bin times). Thus we introduce the approximation expressed in Equation (22):

$$\Gamma(\tau) \approx \Gamma_{Diff}(\tau)\Gamma_{Trip}(\tau) \quad (22)$$

At short bin times, the PCH model must be corrected for the dead time of the photodetector [see Eq. (6)] to retrieve the proper PCH parameters, whose values do not depend on the dead time. Therefore, the resulting PCMH curves are identical to those produced by an ideal photodetector ($\tau_{Dead} = 0$), and Equations (15) and (16) are still valid.

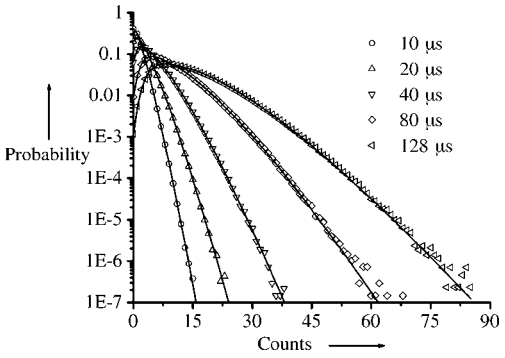

Figure 1. *Photon counting histograms at different bin times. Data are taken from a solution of TMR (≈4 nM) in Tris buffer (50 mM, pH 8.0). Laser power is ≈75 μW at the sample. Representative bin times shown are 10 ($\chi^2 = 1.8$), 20 ($\chi^2 = 1.0$), 40 ($\chi^2 = 0.9$), 80 ($\chi^2 = 1.4$), and 128 μs ($\chi^2 = 1.2$).*

Table 1. *PCMH analysis for data in Figure 3. The autocorrelation function G(T) is fitted to a model describing the 3D diffusion of a single species. $\bar{N}(0)$ is the true average number of molecules in the observation volume, and $\varepsilon_{sec}(0)$ is the true specific brightness (in kilocounts per second per molecule, or kcpsm). τ_{Diff} is the diffusion time (in microseconds) of the species in the observation volume. $\kappa = 6.2 \pm 0.9$ is obtained from the autocorrelation function and fixed to this value for the fit of both PCMH curves.*

Function	$\bar{N}(0)$	$\varepsilon_{sec}(0)$ [kcpsm]	τ_{Diff} [μs]
PCMH $\varepsilon_{sec}(T)$	–	188.7 ± 0.3	55.4 ± 0.4
PCMH $\bar{N}(T)$	2.255 ± 0.005	–	59.72 ± 0.07
FCS $G(T)$	2.225 ± 0.003	–	58.1 ± 0.6

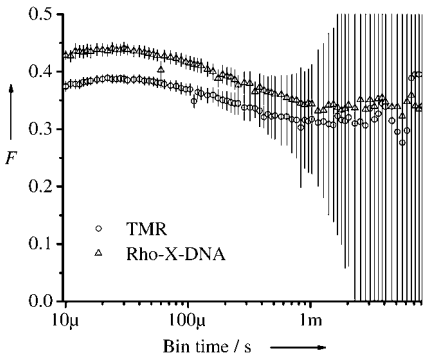

Figure 2. *The variation in F is shown for two samples: TMR (2 nM) and Rho-X-DNA (4 nM). Laser power is ≈75 μW at the sample.*

Results and Discussion

The Effect of Bin Time on PCH for One-Photon Excitation

To examine the bin time effect on PCH, we rebinned the same data set obtained from a sample of tetramethylrhodamine-5-maleimide (TMR) with different bin times T to produce the histograms shown in Figure 1. Even at bin times much longer than the characteristic diffusion time shown in Table 1 ($\tau_{Diff} =$ 58.1 μs), the PCH model is still able to describe the experimental histograms, as demonstrated by the goodness of each fit and a relatively constant value of F (see Figure 2). Therefore the concept of apparent specific brightness, $\varepsilon_{sec}(T)$, and apparent average number of molecules, $\bar{N}(T)$, is practicable in PCH analysis.

When $\bar{N}(T)$ and $\varepsilon_{sec}(T)$ extracted from each histogram in Figure 1 are plotted against the bin time, they begin to vary significantly on a time scale similar to the diffusion time of the fluorescent species. This variation continues over several orders of magnitude (see Figure 3). Using a single-species model of diffusion [see Eq.(17)], Equations (15) and (16) can successfully fit $\varepsilon_{sec}(T)$ (in counts per second per molecule) and $\bar{N}(T)$ as a function of the bin time. By performing such a fit, we extrapolate to $T = 0$ and recover a true specific brightness, $\varepsilon_{sec}(0)$ (in kilocounts per second per molecule, or kcpsm), and a true average number of particles, $\bar{N}(0)$, that are independent of bin time. For a sample of TMR, the fitting parameters recov-

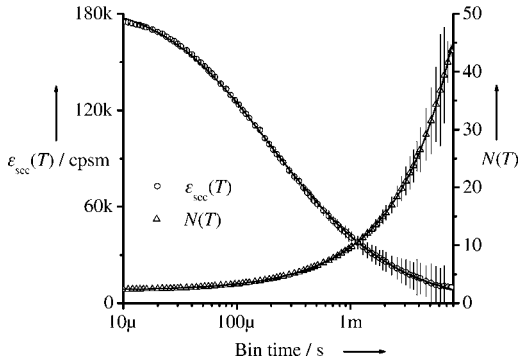

Figure 3. *Variation of apparent* $\bar{N}(T)$ *and* $\varepsilon_{sec}(T)$ *for the same sample used in Figure 1.* $\varepsilon_{sec}(T)$ *and* $\bar{N}(T)$ *are fit to Equations (15) and (16) respectively. Table 1 presents the numerical results of each fit.*

ered from the apparent specific brightness shown in Figure 3 are $\varepsilon_{sec}(0) = 188.7 \pm 0.3$ kcpsm and $\tau_{Diff} = 55.4 \pm 0.4$ µs. Likewise, fitting Equation (16) to the apparent average number of molecules gives the results $\bar{N}(0) = 2.255 \pm 0.005$ molecules and $\tau_{Diff} = 59.72 \pm 0.07$ µs. The fit to the autocorrelation function for a single species undergoing three-dimensional diffusion yields the following fitting parameters: $\bar{N}_0 = 2.225 \pm 0.003$ molecules and $\tau_{Diff} = 58.1 \pm 0.6$ µs. Overall the parameters determined from different procedures are in good agreement, demonstrating the validity of PCH fitting at multiple bin times.

When the fitted *F* is plotted against the bin time (see Figure 2), its value decreases slightly with increasing bin time. *F* starts at 0.39 for 10 µs and finishes at 0.30 for 7.68 ms. As shown in Figure 2, the variation of the *F* factor does not seem to depend on the diffusion time of the species under consideration. Rho-X-DNA, which is a 12-mer of single-stranded DNA labeled with Rhodamine-X ($\tau_{Diff} = 105$ µs), has a longer diffusion time than TMR ($\tau_{Diff} = 58.1$ µs). The *F* factor for both samples differs only slightly in its amplitude. According to Equations (15) and (16), *F* fixed to a certain value should not affect the diffusion time. Table 2 shows nearly constant diffusion

Table 2. *Diffusion time of TMR with different values of* F. *The diffusion times (in microseconds) are obtained from the same data set shown in Table 1. During the fitting procedure,* κ *is fixed to a value of 6.2 [see Table 1].*

Function	*F* varied	$F = 0.39$	$F = 0.35$	$F = 0.30$
PCMH $\varepsilon_{sec}(T)$	55.4 ± 0.4	60.33 ± 0.07	60.4 ± 0.1	60.1 ± 0.1
PCMH $\bar{N}(T)$	59.72 ± 0.07	60.41 ± 0.08	60.4 ± 0.1	59.7 ± 0.1

times for TMR obtained from PCMH curves with different values of *F* (allowed to vary, and fixed to 0.39, 0.35, and 0.30). Therefore, the correction to the non-Gaussian observation volume profile using the semi-empirical factor *F* is robust.

Let us try to understand the physical meaning behind the variation of both PCH parameters with bin time. In Equation (1), the molecular brightness is multiplied by the actual observation volume profile, $W(\vec{r})$, which is a function of the position of the particle within the volume of reference $\vec{r}$. For short bin times, the particle is approximated as being stationary, and thus the vector $\vec{r}$ is constant. With increasing bin times, the position of the particle can no longer be approximated as fixed. Because the particle diffusion is governed by Brownian motion (modeled as a random walk), the positional distribution is a 3D Gaussian function (integral normalized to unity) with a time-dependent width. The integral in Equation (1) can be imagined as a convolution of the actual observation volume profile with this 3D Gaussian function. As the bin time increases, the width of this 3D Gaussian function also increases, thus decreasing its amplitude at the center. Because the molecular brightness is defined at the center of the observation volume, the apparent specific brightness decreases with increasing integration time. In other words, at short bin times, $\varepsilon_{sec}(T)$ can be qualitatively described as a bright point positioned at the center of the observation volume. With increasing bin time, $\varepsilon_{sec}(T)$ becomes a blurrier and dimmer spot spread over an increasing volume. The same reasoning can be applied for the average number of molecules. At short bin times, $\bar{N}(T)$ represents the true average number of molecules within the observation volume. As the bin time increases, the number of particles able to diffuse into the volume becomes larger.

As previously shown, *F* decreases slightly with increasing bin time. This decrease indicates that with larger bin times, the actual volume of observation becomes closer to a 3D Gaussian volume (by definition). Indeed, as the bin time increases, the actual observation volume profile becomes more Gaussian when convoluted with an increasingly broad time-dependent 3D Gaussian function.

To avoid significant deviation from the true values of the PCH parameters, the bin time chosen should be smaller than the diffusion time of the analyte. Using Equation (15), we can actually quantify this deviation when the diffusion time is known. For example, to ensure a deviation in specific brightness smaller than 10%, a bin time shorter than 34% of the diffusion time should be used. When the diffusion time is unknown, we can use PCMH to determine both the time-independent parameters, $\varepsilon_{sec}(0)$ and $\bar{N}(0)$, and the time-dependent parameter, τ_{Diff}. In the section after next, we discuss the minimum bin time needed to avoid further deviations from additional fluctuation processes.

FCS alone cannot recover the true specific brightness, $\varepsilon_{sec}(0)$, by simply dividing the average fluorescence intensity $\langle I \rangle$ by $\bar{N}(0)$ [Eqs. (8) and (13)]. The reason why this approach fails is that γ_2 cannot be determined using the standard 3D Gaussian approximation for the observation volume.[20] We have previously shown that γ_2 depends on the semi-empirical factor *F* and can be measured using PCH.[1]

Determining Diffusion Times for Multiple Species Using PCMH

To demonstrate that PCMH can resolve a mixture of fluorescent species by molecular brightness and still recover their diffusion times, we measured the PCMH curves, $\bar{N}(T)$ and $\varepsilon_{sec}(T)$, and the autocorrelation function, $G(T)$, of two different samples: Cy3-maleimide (Cy3) and Rho-X-DNA. We then mixed

equal volumes of the two samples and obtained their PCMH curves as well as the autocorrelation function.

For each species, we compared the fitting parameters obtained from $\varepsilon_{sec}(T)$, $\bar{N}(T)$, and $G(T)$ for both the one-species and two-species samples. Figure 4 illustrates the apparent specific brightness, $\varepsilon_{sec}(T)$, for Cy3 and Rho-X-DNA in the two-species sample for bin times from 10 μs to 5.12 ms. The true specific brightness $\varepsilon_{sec}(0)$ of each species remains constant between

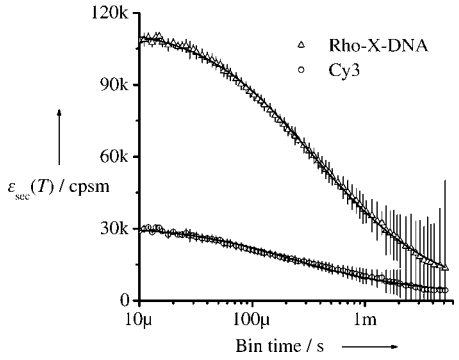

Figure 4. *Variation of apparent $\varepsilon_{sec}(T)$ for a mixture of Rho-X-DNA (2 nM) and Cy3 (5 nM) diffusing through a confocal volume. Laser power is ≈75 μW at the sample. Table 3 presents the numerical results of each fit.*

the one- and two-species samples, as expected (see Table 3). For both one-species samples, the true average number of molecules $\bar{N}(0)$ is in good agreement with the parameter obtained from the autocorrelation function for both Cy3 and Rho-X-DNA. In the two-species sample, we expect these numbers to be halved because each species was mixed in equal amounts by volume. Instead the experimental data show that $\bar{N}(0)$ for Cy3 is slightly higher than expected, whereas $\bar{N}(0)$ for Rho-X-DNA is lower.

The discrepancy in $\bar{N}(0)$ probably arises from small differences in the magnitude of F for each species. Thus it is necessary to fix F during the fit of individual PCHs when constructing a PCMH for a mixture of species. For the two-species sample shown in Table 3, we set F to the average value for both samples at $T = 10$ μs ($F = 0.42$). Nevertheless the small variation in F between the two fluorescent species does not affect the ability of the model to distinguish between one and two species. When a one-species model is used to fit a two-species sample, F goes to unreasonable values for the configuration of our confocal microscope ($F > 1$).[1]

As demonstrated earlier, differences in F affect only $\varepsilon_{sec}(0)$ and $\bar{N}(0)$. Indeed the diffusion times determined by PCMH for both the one- and two-species samples are in good agreement with those obtained from the autocorrelation function of the one-species samples. While PCMH can determine the diffusion time of each species in the two-species sample, FCS cannot be fit with a model for two diffusing species. This is the case even when the parameters for one species are fixed to their true values. We conclude that FCS cannot resolve Cy3 and Rho-X-DNA in the mixed sample because the difference in diffusion time is too small.

Müller, Chen, and Gratton[21] found that the resolution of PCH depends on the signal statistics, the absolute molecular brightness, the average number of molecules, and the brightness ratio of the two species. As a technique built upon the PCH model, the resolving power of PCMH is determined by the brightness ratio of the species present in the sample. Figure 4 shows that the apparent specific brightness of a species varies according to its diffusion time. Thus for a two-species sample with different diffusion times, the apparent brightness ratio, $\varepsilon_{sec,bright}(T)/\varepsilon_{sec,dim}(T)$, will vary with bin time.

Let us consider three cases: 1) A sample with a bright-slow species and a dim-fast species (Figure 5A). When the bin time increases, the apparent specific brightness of the dim species will drop more rapidly because of its faster diffusion, thus increasing the brightness ratio and resolution of PCH fitting at longer bin times. 2) A sample with a bright-fast species and a dim-slow species (Figure 5B). In this case, the apparent specific brightness of the bright species drops more rapidly than that of the dim species. The PCMH curves of these two species may cross at a certain bin time (where the PCH model can detect only one species). At longer bin times, these curves will separate again. Thus, the PCMH analysis is still practicable when the crossing region is excluded from the fitting. 3) A sample with two species that have similar diffusion times but different brightnesses (Figure 5C). In this case, the apparent brightness ratio of the two species does not change with the bin time. Thus, the resolution of PCH analysis depends on their true brightness ratio only. If this ratio is too small (usually a minimum ratio of two is required for resolving species[21]), the PCH model will detect only one species at any given bin time and the PCMH curves cannot be determined.

Table 3. *PCMH analysis for data in Figure 4. The top six rows show the data obtained for Cy3 alone and mixed with Rho-X-DNA. The bottom six rows show the data obtained for Rho-X-DNA alone and mixed with Cy3. During the fitting procedure, κ is fixed to a value of 6.2 [see Table 1].*

Sample	Function	$\bar{N}(0)$	$\varepsilon_{sec}(0)$ [kcpsm]	τ_{Diff} [μs]
Cy3	PCMH $\varepsilon_{sec}(T)$	–	29.4 ± 0.1	54.6 ± 0.9
One species	PCMH $\bar{N}(T)$	6.62 ± 0.02	–	54.7 ± 0.9
	FCS $G(T)$	6.8 ± 0.1	–	58 ± 2
Cy3	PCMH $\varepsilon_{sec}(T)$	–	27.9 ± 0.3	61 ± 3
Two species	PCMH $\bar{N}(T)$	3.56 ± 0.03	–	62 ± 3
	FCS $G(T)$	–	–	–
Rho-X-DNA	PCMH $\varepsilon_{sec}(T)$	–	114.2 ± 0.2	103 ± 1
One species	PCMH $\bar{N}(T)$	2.508 ± 0.005	–	100 ± 1
	FCS $G(T)$	2.55 ± 0.02	–	105 ± 1
Rho-X-DNA	PCMH $\varepsilon_{sec}(T)$	–	111.8 ± 0.3	97 ± 2
Two species	PCMH $\bar{N}(T)$	0.89 ± 0.01	–	96 ± 5
	FCS $G(T)$	–	–	–

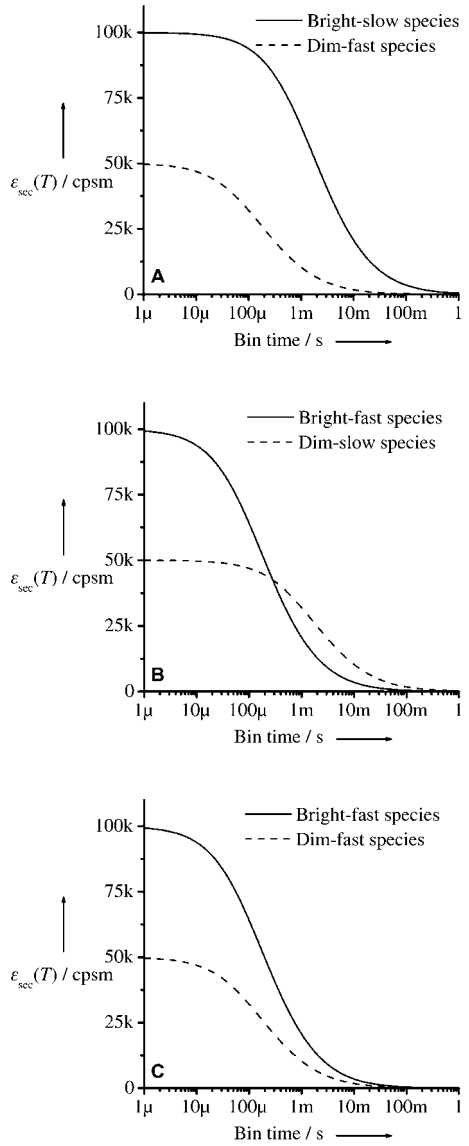

Figure 5. *Theoretical PCMH curves determined by Equation (15) for a sample containing two different types of species: A) bright-slow and dim-fast; B) bright-fast and dim-slow; and C) bright-fast and dim-fast, which is equivalent to bright-slow and dim-slow. A bright species is defined as $\varepsilon_{sec}(0) = 100$ kcpsm and a dim species as $\varepsilon_{sec}(0) = 50$ kcpsm. A fast species is defined as $\tau_{Diff} = 50$ µs and a slow species as τ_{Diff} of 500 µs.*

Analyzing Additional Fluctuation Processes

To determine whether information could be extracted for faster fluctuation processes such as triplet-state formation, we extended the PCMH curves in Figure 3 to 2 µs. At such short bin times, the effect of detector dead time becomes significant. Indeed, if the PCH parameters are extracted using the ideal photodetector model [see Eq. (3)], $\varepsilon_{sec}(T)$ starts to decrease rapidly and $\bar{N}(T)$ to increase as T approaches zero. These results are consistent with the ones previously reported.[17] Using the same procedure as Hillesheim and Müller,[17] we measured a dead time for our photodetector of $\tau_{Dead} = 42.5 \pm 0.6$ ns, consistent with the specification given by the manufacturer. Once the PCH parameters are extracted with the dead-time-modified PCH model [see Eq. (6)], the PCMH curves are fit to Equations (15) and (16) as shown in Figure 6 (for $\varepsilon_{sec}(T)$ and $\bar{N}(T)$ respectively). The results, which are shown in Table 4, illustrate a good agreement for τ_{Trip} and F_{Trip} whether they are extracted from the PCMH curves or from the autocorrelation function. While the PCMH curve is only extended to 2 µs, a τ_{Trip} of 2 µs can still be determined with confidence. Because the PCMH curve is a double integration of the FCS function, Equation (21) drops to half of its amplitude at the bin time that is about three times as long as the triplet relaxation time. Although the F factor is stable (0.39) at bin times lower than 10 µs, F increases slightly at high laser power ($F = 0.45$ at approximately 200 µW). This effect can be explained as follows: because triplet-state formation depends on the excitation intensity, its contribution is not constant over the entire observation volume profile (higher at the center and lower at the edge). Thus, the actual observation volume profile becomes less Gaussian-like and the F factor increases. This fact cautions

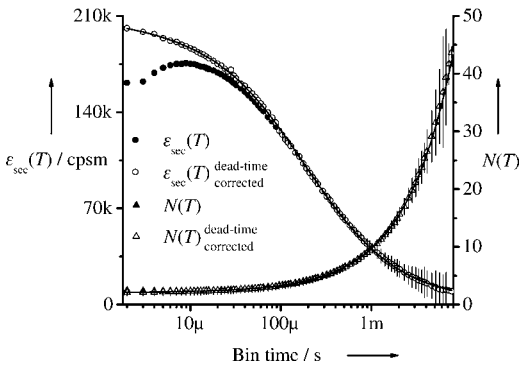

Figure 6. *To include additional fast fluctuation processes, the variation of $\bar{N}(T)$ and $\varepsilon_{sec}(T)$ is measured at short bin times for the same sample under the same experimental conditions as in Figure 3. At short bin times (< 10 µs), the effect of dead time becomes clear for both PCH parameters. When the detector is considered as ideal, $\varepsilon_{sec}(T)$ starts to decrease whereas $\bar{N}(T)$ starts to increase. Once the PCH parameters are obtained from the dead-time-modified PCH model using Equation (6), $\varepsilon_{sec}(T)$ and $\bar{N}(T)$ are fitted to Equations (15) and (16) respectively. Table 4 presents the numerical results of each fit.*

Table 4. *PCMH analysis for data in Figure 6. The fluorescence autocorrelation function $G(T)$ is fitted to a model describing the three-dimensional diffusion with triplet-state formation of a single species. τ_{Trip} represents the relaxation time (in microseconds) between the dark state and the bright state, and F_{Trip} (in percent) is defined as the average fraction of dark molecules. $\kappa = 4.6 \pm 0.7$ obtained from the autocorrelation function is fixed to this value during the fit of each PCMH curve.*

Function	$\bar{N}(0)$	$\varepsilon_{sec}(0)$ [kcpsm]	τ_{Diff} [µs]	τ_{Trip} [µs]	F_{Trip} [%]
PCMH $\varepsilon_{sec}(T)$	–	191.3 ± 0.8	57.0 ± 0.8	2.1 ± 0.6	6.0 ± 0.5
PCMH $\bar{N}(T)$	2.230 ± 0.004	–	57.6 ± 0.4	1.6 ± 0.3	7.9 ± 0.4
FCS $G(T)$	2.259 ± 0.007	–	61 ± 1	1.8 ± 0.3	6.3 ± 0.7

us to avoid high laser power when using the PCH model for one-photon excitation.

Using Equation (21), we are able to quantify the influence of additional fluctuation processes on the value of PCH parameters with a certain bin time. For example, in a system with a triplet fraction of 20% and triplet relaxation time of 2 μs, the bin time for PCH analysis has to be at least 7 μs to keep the influence of triplet formation on the fitted brightness below 10%. PCH analysis using a bin time that is longer than this value will return an averaged brightness for molecules switching between the singlet and triplet states and the average number of molecules in both states. If the triplet fraction is small ($<10\%$), its influence can be safely ignored even at short bin times.

Conclusions

We have demonstrated the validity and robustness of our one-photon excitation PCH model with multiple bin times. We have shown that the semi-empirical parameter *F* introduced in the one-photon PCH model varies slightly with increasing bin times and with increasing triplet-state formation. This variation is consistent with the definition of *F,* thus reinforcing the physical interpretation of this parameter as a deviation from the three-dimensional Gaussian volume. Although *F* changes with increasing bin time, this variation is small compared to the variation induced by fitting the histogram with an incorrect number of species. Hence *F* remains a robust semi-empirical parameter for the one-photon excitation PCH model. We have also shown that by varying the bin time, PCMH can extract time-independent parameters (such as the true specific brightness and the true average number of molecules), and time-dependent parameters (such as the diffusion time and the triplet-state relaxation time) from the same set of data. Additionally we have shown that PCMH can recover the diffusion time for each species in a two-species sample even when FCS cannot. This study has established practical limits on applying PCH and PCMH for one-photon excitation.

Experimental Section

Instrumentation: The confocal microscope used in all experiments is similar to that described previously,[1] with the following modifications. All experiments were performed with a water immersion objective (Plan Apo 60X NA = 1.20, Nikon, USA) and a 50 μm pinhole. An additional dichroic mirror (630DRLP, Omega Optical, USA) was added between the pinhole and the emission filter. The autocorrelation function was obtained from a digital correlator (Flex99R-480, Correlator.com, Bridgewater, NJ). The data acquisition time is 500 seconds for the TMR sample and 1000 seconds for the Cy3 and Rho-X-DNA mixed sample.

Sample Preparation: Tetramethylrhodamine-5-maleimide (TMR) was purchased from Molecular Probes (Eugene, OR). Cy3-maleimide (Cy3) was purchased from Amersham Biosciences (Piscataway, NJ). Rhodamine Red-X single-stranded DNA (5′-RhoR-X-CCG CCG TAT CGC C-3′) was purchased from Integrated DNA Technologies (Coralville, IA).

Data Analysis: The reconstruction of the photon count time trace for a given bin time *T* and the determination of the resulting PCH parameters are similar to those described previously.[1] All PCMH curves were fitted using a Marquardt–Levenberg least square algorithm in Origin Pro 7.0 (OriginLab, USA). The errors are estimated by the fitting procedure.

Acknowledgements

T.D.P. is grateful for a Franklin Veatch Memorial Scholarship and B.H. is grateful for a Stanford Graduate Fellowship. The authors thank Michael P. Bokoch, who suggested several improvements in the original manuscript. This work is supported by the National Science Foundation under NSF MPS-0313996.

Keywords: confocal microscopy · few-molecule spectroscopy · fluorescence spectroscopy · photon counting histogram · single-molecule studies

[1] B. Huang, T. D. Perroud, R. N. Zare, *ChemPhysChem* **2004**, *5*, 1523 – 1531.
[2] L. Edman, R. Rigler, *Proc. Natl. Acad. Sci. USA* **2000**, *97*, 8266 – 8271.
[3] S. Wennmalm, L. Edman, R. Rigler, *Proc. Natl. Acad. Sci. USA* **1997**, *94*, 10641 – 10646.
[4] U. Haupts, S. Maiti, P. Schwille, W. W. Webb, *Proc. Natl. Acad. Sci. USA* **1998**, *95*, 13573 – 13578.
[5] P. Schwille, J. Korlach, W. W. Webb, *Cytometry* **1999**, *36*, 176 – 182.
[6] T. Wohland, K. Friedrich, R. Hovius, H. Vogel, *Biochemistry* **1999**, *38*, 8671 – 8681.
[7] J. Widengren, R. Rigler, *Cell. Mol. Biol.* **1998**, *44*, 857 – 879.
[8] S. T. Hess, S. H. Huang, A. A. Heikal, W. W. Webb, *Biochemistry* **2002**, *41*, 697 – 705.
[9] N. L. Thompson in *Topics in Fluorescence Spectroscopy, Vol.* 1 (Ed.: J. R. Lakowicz), Plenum Press, New York, London, **1991**, pp. 337 – 378.
[10] H. Qian, E. L. Elson, *Biophys. J.* **1990**, *57*, 375 – 380.
[11] H. Qian, E. L. Elson, *Proc. Natl. Acad. Sci. USA* **1990**, *87*, 5479 – 5483.
[12] Y. Chen, J. D. Müller, P. So, E. Gratton, *Biophys. J.* **1999**, *77*, 553 – 567.
[13] P. Kask, K. Palo, D. Ullmann, K. Gall, *Proc. Natl. Acad. Sci. USA* **1999**, *96*, 13756 – 13761.
[14] J. D. Müller, *Biophys. J.* **2004**, *86*, 3981 – 3992.
[15] T. D. Perroud, B. Huang, M. I. Wallace, R. N. Zare, *ChemPhysChem* **2003**, *4*, 1121 – 1123; corrigendum in *ChemPhysChem* **2003**, *4*, 1280, 4.
[16] K. Palo, U. Metz, S. Jager, P. Kask, K. Gall, *Biophys. J.* **2000**, *79*, 2858 – 2866.
[17] L. N. Hillesheim, J. D. Müller, *Biophys. J.* **2003**, *85*, 1948 – 1958.
[18] B. Saleh in *Photoelectron statistics*, *Vol.* 6 (Ed.: D. L. MacAdam), Springer-Verlag, Berlin, **1978**, pp. 57 – 84.
[19] J. Widengren, U. Mets, R. Rigler, *J. Phys. Chem.* **1995**, *99*, 13368 – 13379.
[20] S. T. Hess, W. W. Webb, *Biophys. J.* **2002**, *83*, 2300 – 2317.
[21] J. D. Müller, Y. Chen, E. Gratton, *Biophys. J.* **2000**, *78*, 474 – 486.

Received: November 19, 2004
Revised: March 3, 2005

